Contribution of deep convection in the intensification of Mediterranean Tropical-Like Cyclones

Dafis S., Claud C., Kotroni V., Lagouvardos K., Rysman J.F.

Contact: stavros.dafis@lmd.ipsl.fr

LMD/IPSL, CNRS UMR 8539, École Polytechnique, Palaiseau, France and National Observatory of Athens, Greece (NOA/IERSD)

The **Mediterranean Tropical-Like Cyclones (medicanes)** consist of a small fraction of intense marine cyclones which deviate from the classical conceptual models and exhibit characteristics of cyclones with **both extratropical** (e.g., frontal activity) and **tropical characteristics** (e.g., warm core structure and deep convective clouds in spiral forms and/or a central cloud-free "eye"). These cyclones emerge first as extratropical systems that experience intensification periods and hybrid characteristics (extratropical and tropical). Both **baroclinic instability and convection act in synergy to intensify medicanes** but the processes that play the primary role at each of their development stages and intensification periods, remain an open question.

The present work focuses on the **diabatic processes during deep convection (DC)** activity in medicanes to better understand the processes leading to cyclone intensification periods.

Fig. 1 Medicane IANOS, 17 September 2020 (Image courtesy: NASA)

Contribution of deep convection in the intensification of Mediterranean Tropical-Like Cyclones

1. Passive microwave satellite observations (16 km - 4-5 times/day)

DC, intense rainfall and convective overshooting top (COV) detection is achieved by using brightness temperatures (BTs) from the **water vapor channels** 183.31±1 GHz (BT_3), 183.31±3 GHz (BT_4), and 183.31±7 / 190.3 GHz (BT_5) of AMSU-B[1] and MHS[2] which are are **very sensitive to high density frozen hydrometeors** (such as graupel and hail).

DC: $BT_3 - BT_5 \geq T_0$ and $BT_3 - BT_4 \geq T_0$ and $BT_4 - BT_5 \geq T_0$

COV: $BT_3 - BT_5 \geq BT_3 - BT_4 \geq BT_4 - BT_5 \geq T_1$

where T_0 and T_1 (K) *depend on the* viewing angle

MR: $BT_3 - BT_5 \geq -8$ K

[1]AMSU-B: Advanced Microwave Sounding Unit onboard NOAA satellites
[2]MHS : Microwave Humidity Sounder onboard NOAA & MetOp satellites
[3]SEVIRI: Spinning Enhanced Visible and Infrared Imager onboard Meteosat satellites

2. Infrared satellite observations (3 km – every 30 minutes)

In order to detect DC and COV using SEVIRI[3] we use **channel differencing** between the water vapor channel **WV6.2** and the window channel **IR10.8** (ΔBT).

During intense DC important amounts of water vapor can be transported in the lower stratosphere where it is **reemitted at higher temperatures in the WV6.2** channel than in the window channel (COV).

DCPIXELS: WV6.2 – IR10.8 > -10 K

COV: WV6.2 – IR10.8 > 0 K

Fig. 3 Infrared BT IR10.8 (K) (grey) and DCPIXELS (K) (blue and red) derived from SEVIRI (Meteosat-11) during Medicane ZORBAS on 28/09/2018 at 0830 UTC. Overlapped dots: diagnostics for deep convection (DC) from the microwave sounder MHS on-board MetOp-B (green), convective overshooting (COV) (white asterisks) and the scanning footprint (orange) at 0833 UTC. The red circles enclose disks within 200 km from the centre of the cyclone (red asterisk) every 50 km. →

Fig. 2 Deep moist convection with overshooting tops as seen from space. Image courtesy: International Space Station (ISS) (ESA/NASA)

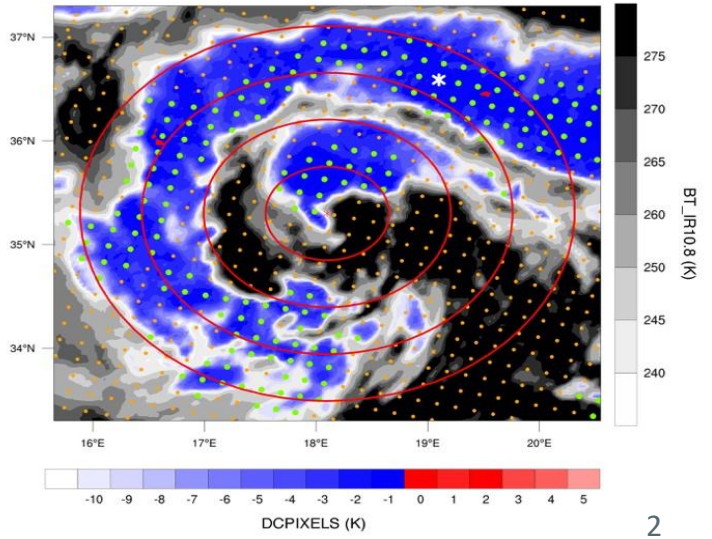

Contribution of deep convection in the intensification of Mediterranean Tropical-Like Cyclones

3. Model analysis (IFS) and Reanalysis (ERA5)

- Minimum sea-level pressure to track cyclone centers
- Deep layer (850-300 hPa) wind shear (DLS):

$$\mathrm{DLS} = \sqrt{(\boldsymbol{u}300 - \boldsymbol{u}850)^2 + (\boldsymbol{v}300 - \boldsymbol{v}850)^2}$$

- Vortex tilt and thermal structure of medicanes based on vorticity

4. High-resolution modeling with WRF-ARW (3 km)

- DC definition using simulated reflectivity and ice-water content
- Assessment of the contribution of diabatic processes in the surface pressure tendency (PTE)
- Online potential vorticity tracers (PV-tracers)

Numerical simulations of **9 medicanes** were first **evaluated based on satellite observations** before further analysis. **Only 6 simulations had a reasonable representation of the observed DC activity and medicane tracks**.

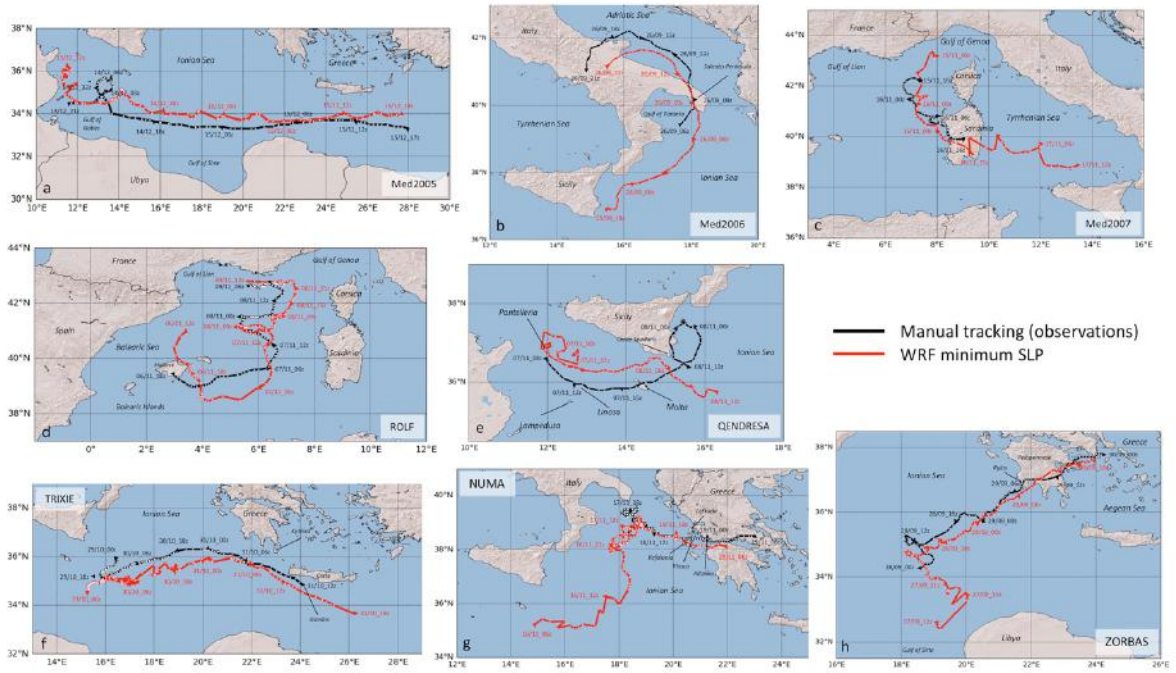

Fig. 4 The observed cyclone tracks (black) (position with white dots) and the tracks based on the position of minimum SLP from WRF plotted every 30 minutes (red).

Contribution of deep convection in the intensification of Mediterranean Tropical-Like Cyclones

Results

1. Case study: ROLF

Dafis, S., Rysman, J.F., Claud, C., and Flaounas, E. (2018) Remote sensing of deep convection within a tropical-like cyclone over the Mediterranean Sea. *Atmospheric Science Letters,* 19. https://doi.org/10.1002/asl.823

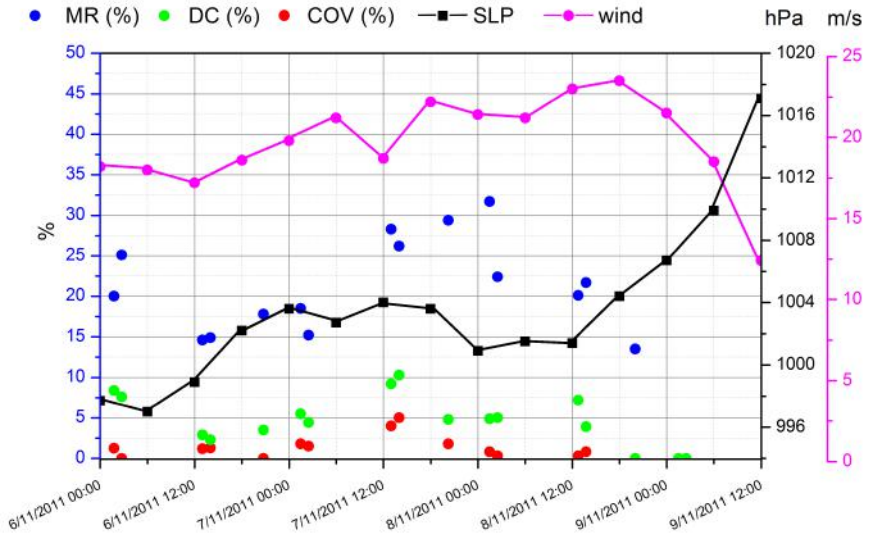

Fig. 5 Time-series of microwave satellite diagnostics occurrence in % for DC (green dots), moderate rainfall (MR) (blue dots), convective overshooting (COV) (red dots) five times per day. Sea-level pressure (SLP-hPa) (black line) and maximum wind speed (m/s) (magenta line from the Integrated Forecasting System (IFS) every 3 hours.

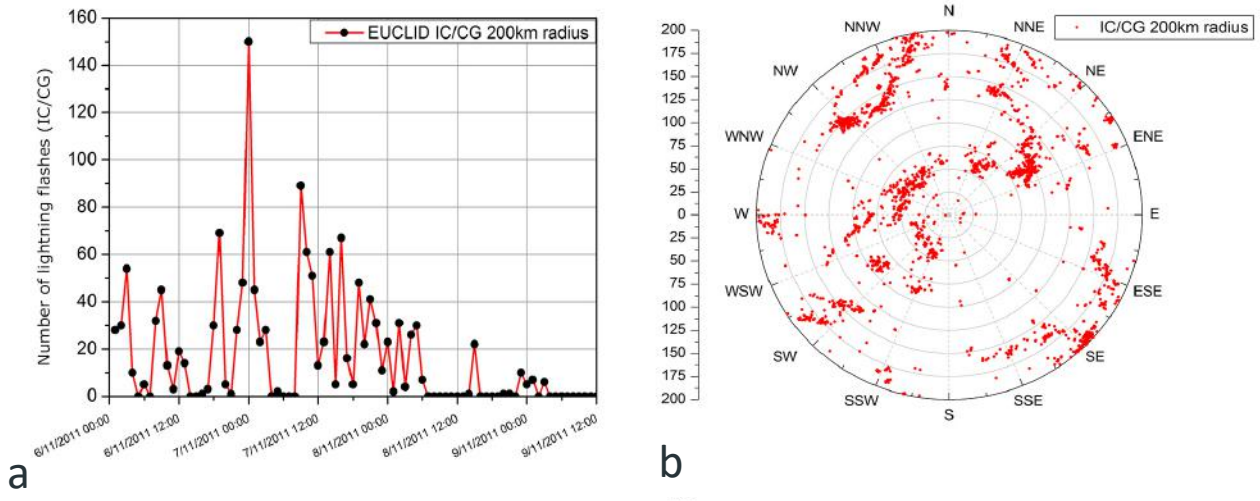

Fig. 6 (a) Hourly lightning flashes (CG & IC) as detected by the European Cooperation for Lightning Detection system. (b) Azimuthal distribution of lightning flashes within a 200 km distance from ROLF's center between 00z on 6 November and 12z on November 9, 2011.

Contribution of deep convection in the intensification of Mediterranean Tropical-Like Cyclones

Results
2. Additional case studies

Dafis, S., Claud, C., Kotroni, V., Lagouvardos, K., and Rysman, J.F. (2020) Insight into the convective evolution of Mediterranean tropical-like cyclones. *Quarterly Journal of the Royal Meteorological Society*. https://doi.org/10.1002/qj.3896

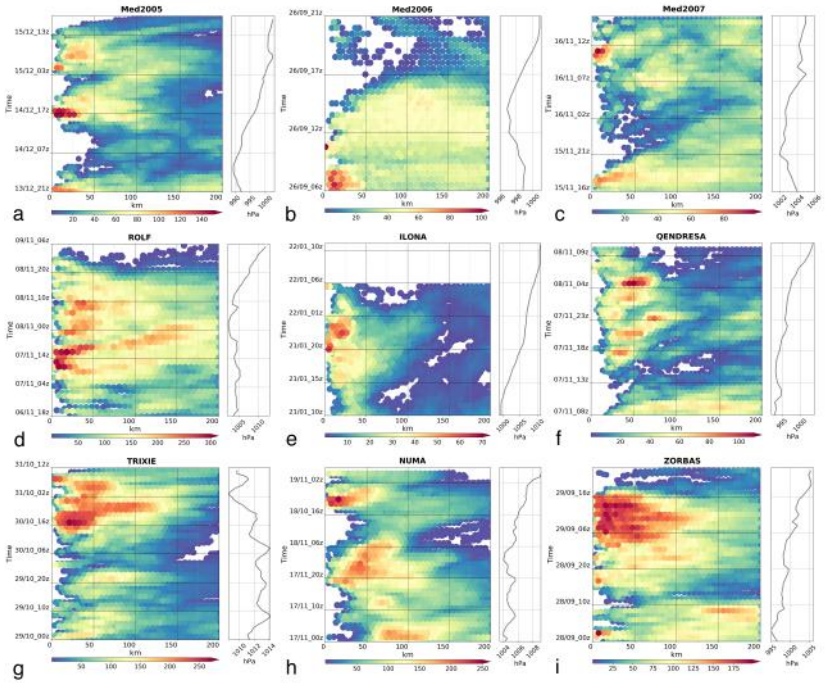

Fig. 7 Composite distribution of aggregated DCPIXELS normalized by the distance from the cyclone centre every 30 minutes and time-series of SLP minima by ERA5 every 1 hour (black line). The shade is the relative occurrence of DC for each individual case (Note that the legend is not the same for each case).

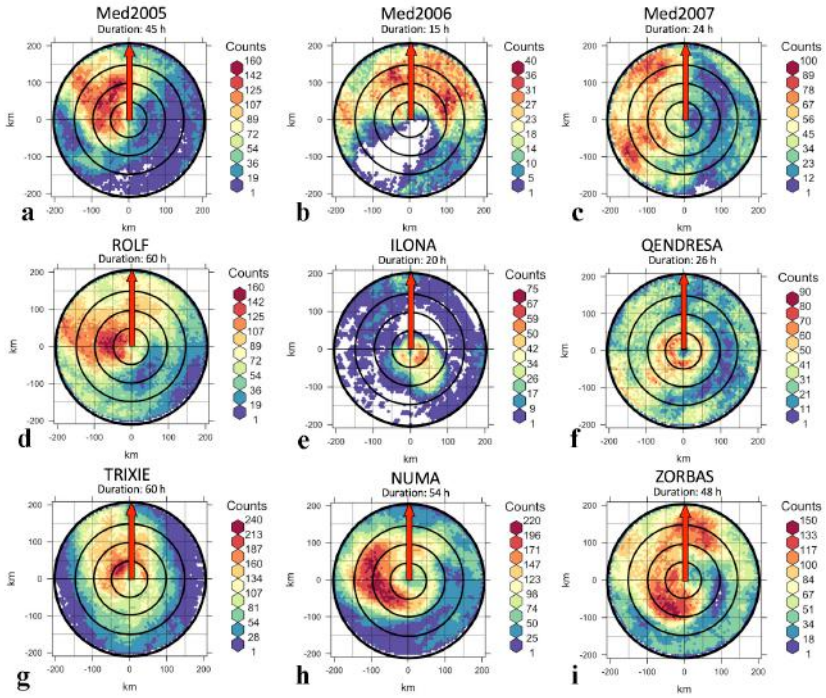

Fig. 8 Composite azimuthal distribution of aggregated DCPIXELS rotated with respect to the DLS vector. The shade is the relative occurrence of DC for each case (Note that the legend is not the same for each case). The red arrow shows the direction of the DLS vector pointing due north.

Results

3. Diabatic contribution to surface pressure tendency and potential vorticity

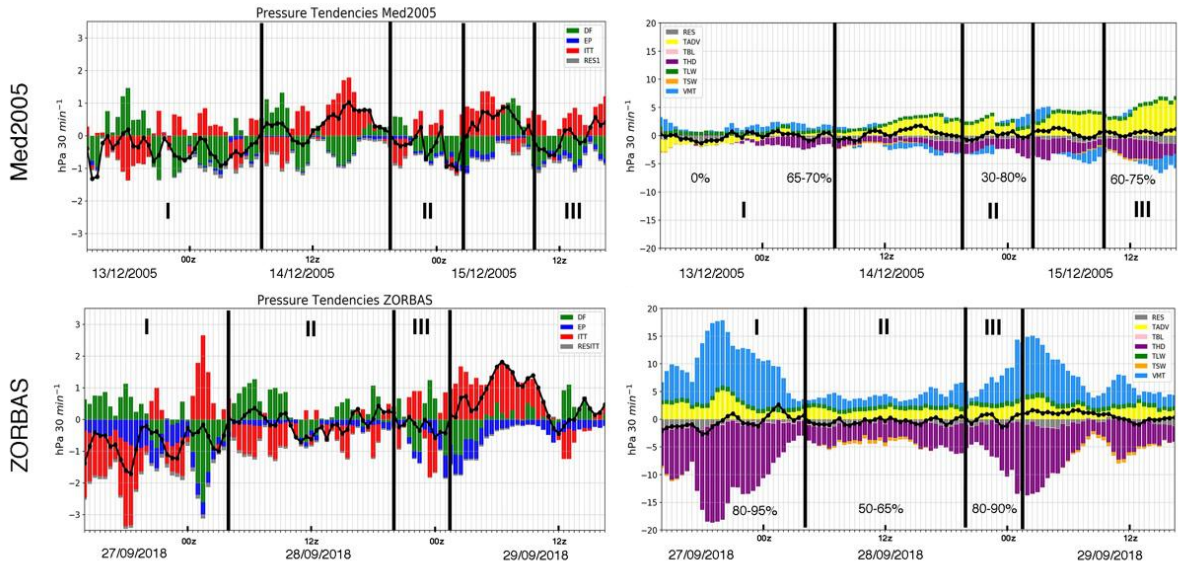

Fig. 9 Time-series for the PTE analysis for a 100 km radius from the center of 2 medicanes: (left column) surface pressure tendency (Dp) (black line), decomposed into contributions by geopotential at 50 hPa (Dϕ), integrated column temperature (ITT) and water loss or gains due to evaporation and rainfall (EP). (Right column) Integrated temperature term (ITT) (black line), decomposed into contributions by vertical movements (VMT), horizontal temperature advection (TADV) and different diabatic heating processes due to the planetary boundary layer (TBL), due to short-wave radiation (TSW), long-wave radiation (TLW) and microphysics (THD). The residuals due to temporal and spatial discretization are shown in grey. The relative contribution of THD to the total negative pressure tendency is shown in percent in the right column. Note the different scale for pressure on the left axis of both columns.

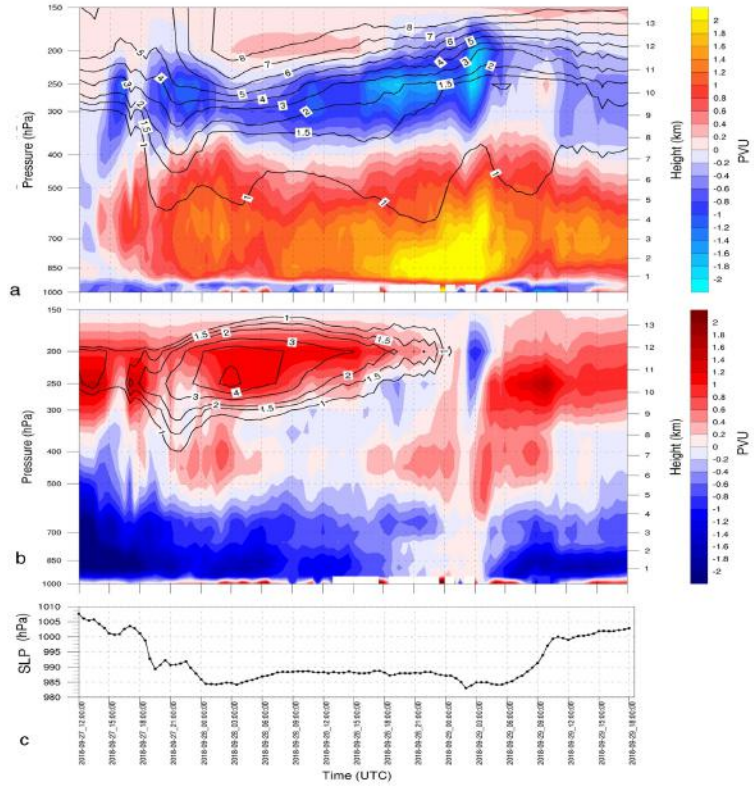

Fig. 10 Time-pressure diagrams for average values within 100 km from the cyclone center of ZORBAS for (a) diabatic PV (shaded, PVU) and large-scale PV (black contours, PVU), and (b) the anomalies of diabatic PV (shaded, PVU) and large-scale PV (black contours-only positive, PVU) with respect to the time of maximum cyclone intensity (minimum SLP shown below in hPa in (c)).

Contact: stavros.dafis@lmd.ipsl.fr

Towards a classification of medicanes

Only a fraction of medicanes experience intensification during DC activity close to their center and upshear convection is linked with rapid intensification periods.

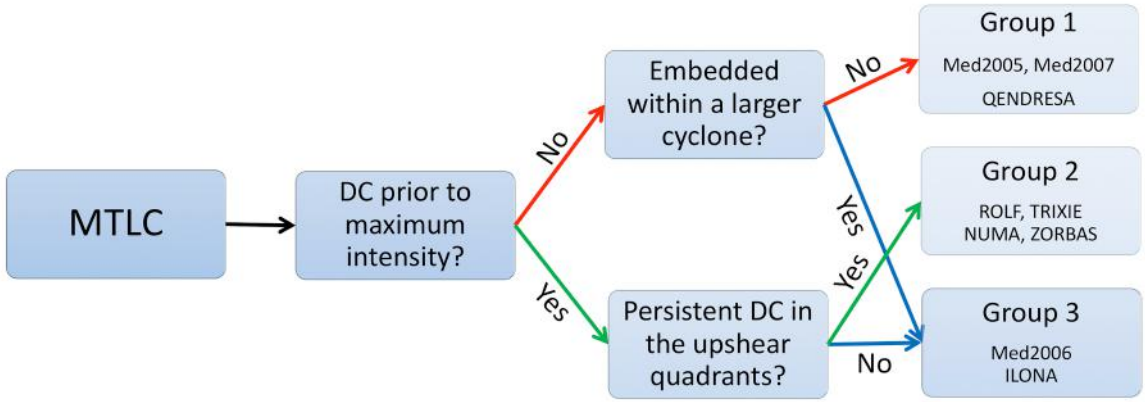

Fig. 11 Decision tree classifier for MTLCs according to DC evolution.

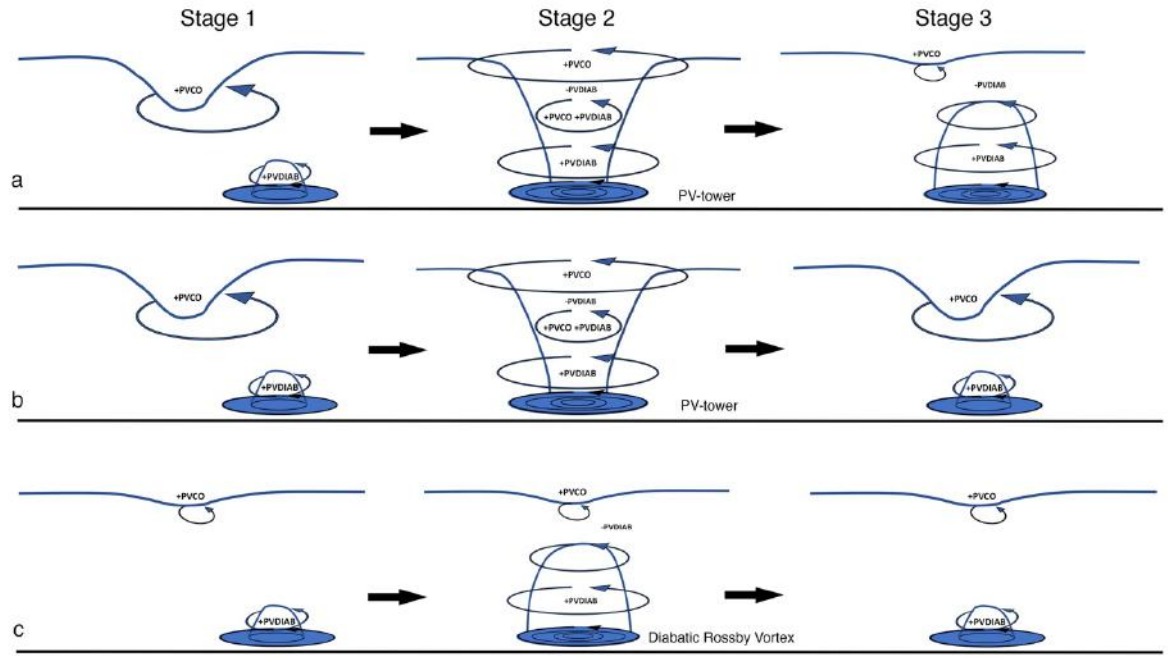

Fig. 12 A schematic diagram of the different stages of the medicanes ZORBAS and NUMA (a), Med2006 (b) and TRIXIE (c). The 2 PVU isoline of the large-scale PV (PVCO) anomaly and the low-level diabatic PV (PVDIAB) anomaly are shown with blue contours. The "+" and "- symbols indicate the sources and sinks of each PV anomaly. Each PV anomaly and its effects are indicated by the size of curved arrows. The induced surface circulation and its relative strength is indicated by the number of enclosed blue circles. The PV-tower and Diabatic Rossby Vortex stages are also indicated and the black arrows show the evolution of each stage.